ORAL REFERENCE: ICF100188OR

SUBCASE CRACK PROPAGATION THRESHOLD AND MICROHARDNESS PROFILE INFLUENCE IN ROLLING CONTACT FATIGUE OF CARBURISED COMPONENTS

G. Donzella, A. Mazzù and L. Solazzi

Dipartimento di Ingegneria Meccanica, Università degli Studi di Brescia,
Via Branze 38, 25073 Brescia, ITALY

ABSTRACT

A new experimental methodology was employed to study the subcase cracks propagation in surface hardened components under rolling contact fatigue: some micro-holes were drilled by electron discharge machining on one of the flat faces of carburised disks, at different depths under the surface. Under cyclic contact tests carried out at different contact pressure levels, some micro-cracks nucleated from the holes border and grew mainly in mode II due to the compressive residual stress state present in the hardened layer. These tests simulate the actual subcase fatigue phenomenon, which starts from inclusions present in the material. The experimental results, calibrated with FEM analyses, gave an indication on the fatigue threshold as a function of defect size and material hardness. The definition of a propagation index allowed to assess the subcase fatigue limit, taking explicitly in to account the hardness profile.

KEYWORDS

Rolling contact fatigue, subcase fatigue, short cracks, hardened components

INTRODUCTION

A lot of components subjected to rolling contact are carburised. This treatment (and generally speaking a surface hardened treatment) limits wear and surface fatigue, so that subsurface fatigue (also said subcase fatigue) becomes more important and probable [1,2]: the cracks propagate almost parallel to the surface in the interface zone between core and hardened case, until they branch and emerge to the surface. In some cases the path covered by the cracks under the surface can be very long, thus producing serious damage at the failure instant.

This paper deals with the evaluation of a threshold of this dangerous damage mechanism in carburised disks, taking in to account the determining role played by the hardness profile along the depth. This role can be understood in a simplified manner, thinking the phenomenon of the subcase fatigue as a competition between contact shear stresses, varying along the depth, and material shear fatigue limit, which depends on the hardness and therefore on the depth again. Some design criteria based on this approach have been proposed in the past. Inherent defects in the material were however recognized to constitute preferential initiation points of subsurface cracks [3,4]: their effect must be therefore taken in to account to predict the development of a subcase fatigue phenomenon. Non-metallic oxide inclusions are particularly dangerous:

they are often present in form of clusters, thus originating greater "SIF equivalent defects". The basis of the work here presented is the short cracks theory. Following this theory, and in particular the Murakami approach [5], the subcase fatigue limit is defined as the propagation threshold of small defects inherent in the material. The results available from the short cracks theory regards however quantitative estimation of mode I threshold: in particular, following the Murakami's relationship, it depends on crack dimension and material hardness in the form:

$$\Delta K_{Ith} \propto (HV + 120) \cdot \left(\sqrt{A}\right)^{1/3} \tag{1}$$

Many difficulties arise in determining the threshold of subcase fatigue cracks, because they propagate mainly in mode II [1,6,7,8] and it is not easy to reproduce this propagation mode in laboratory tests, due to its strong instability [9,10,11]. Some attempts were made on long cracks by Murakami et al. [10] using V-notched cantilever specimens and by Otsuka et al. [6] using clamped specimens. This last work showed in particular that a T-stress (i.e. a compressive stress along the crack direction) acts in stabilising the mode II propagation. A similar condition is present in the rolling contact phenomenon, especially in surface hardened components, were a significant compressive residual stress parallel to the surface is generated by the hardening treatments. The idea followed in the present work was therefore to introduce artificial micro-holes in some carburised disks and to follow their propagation under a RCF test. In such a way, the presence of inherent defects in the material can be simulated, also studying the influence of their dimension and position on the subcase fatigue strength.

EXPERIMENTAL TESTS

The experiment here described was carried out on a carburised disk (120 mm in diameter, 10 mm in thickness) made of 18NiCrMo5 steel, whose hardness profile HV is shown in fig.1.

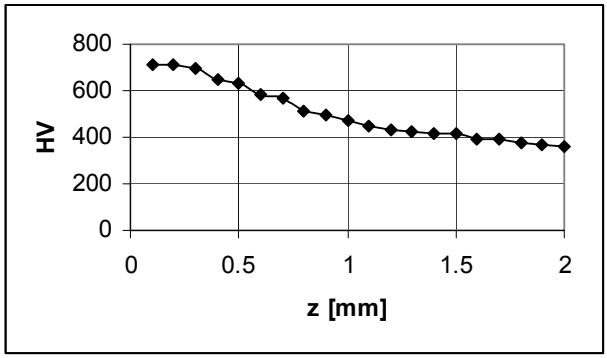

Figure 1: hardness profile of the disk

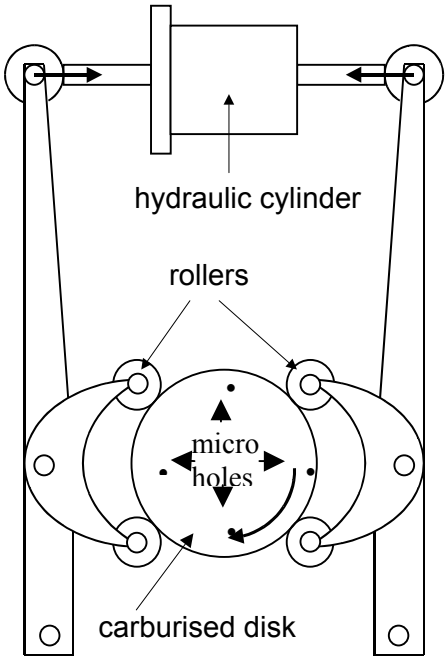

Figure 2: testing apparatus

Four blind micro-holes called A, B, C and D, 130 μm in diameter and 300 μm in length, were machined by electron discharge on one of the flat planes of the disk at different depths z, respectively 250 μm, 380 μm, 510 μm and 620 μm from the surface to the hole axis, in order to study the effect of the hardness gradient. The RCF tests were carried out in pure rolling and lubricated condition with the testing machine, designed at the University of Brescia, schematically shown in fig.2. A constant hertzian pressure p_o was applied during the test, periodically stopping it and examining the disk with an optical microscope. If no crack propagation was detected in $2 \cdot 10^6$ load cycles, the pressure level was incrementally increased by steps of 100 MPa.

NUMERICAL ANALYSES

The aim of the numerical analyses was to calculate the SIFs range during a load cycle for the cracks emanating from the holes, in order to calibrate the experimental results and to determine in this way the correspondent threshold levels. Several plane stress models were employed, simulating the four micro-holes with different crack orientation and length and moving the pressure distribution along the contact surface. The SIFs were calculated from the nodal displacements near the crack tip [12], verifying in every case they respect the singularity field. The submodeling technique, allowed by ABAQUS code, was used for these calculation in order to refine accurately the mesh near the crack tip (fig.3).

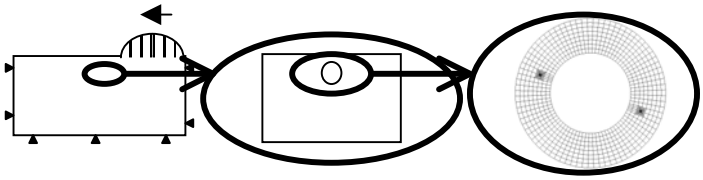

Figure 3: numerical models, using the submodeling technique

RESULTS

No crack propagation from the micro-holes was observed up to a pressure of 2100 MPa. At a pressure of 2200 MPa some micro-cracks started from the holes border. In particolar, from each hole two almost symmetrical cracks appeared, at a direction comprised in the range from 10° to 30° with respect to the surface direction (see fig. 4a). In some cases multiple cracks initiated with various directions, but mainly again in the range from 10° to 30°, as shown in fig. 4b.

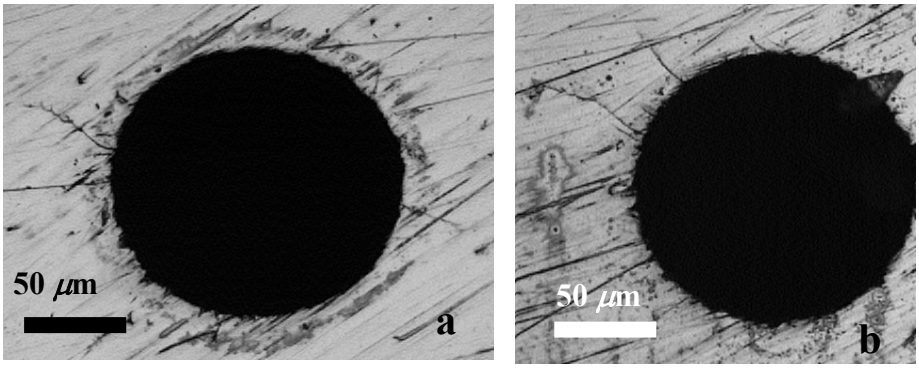

Figure 4: first stage of crack propagation from micro-holes

The numerical analyses showed a clear dominant mode I for the first stage of propagation of these micro-cracks (see fig.5a), but the correspondent calculated SIF is not significant, because near the hole border it is modified by the unknown tensile residual stresses due to electron discharge machining.

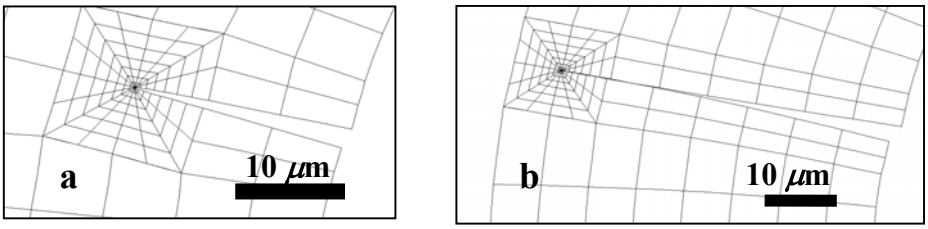

Figure5: deformed meshes of cracks with different length

In the case of multiple cracks, many of these stopped after a few tens of microns (typically 20 μm), going away both from the residual stress zone and from the stress concentration zone around the hole, thus reducing their ΔK_I below ΔK_{Ith}. Only a couple of them for each hole continued growing: the propagation was easier for cracks less inclined with respect to the surface direction. The numerical analyses showed that just for these directions ΔK_{II} reaches its maximum values (see fig. 6) and it increases with the crack length. So, generally speaking we concluded that as a crack starting from the hole border continues growing after 20

μm, the dominating propagation mode in this second stage becomes the mode II, as is also put in evidence by the deformed mesh in fig.5b and by the multiple branching shown in fig.7. A similar result was found numerically by Melander [13].

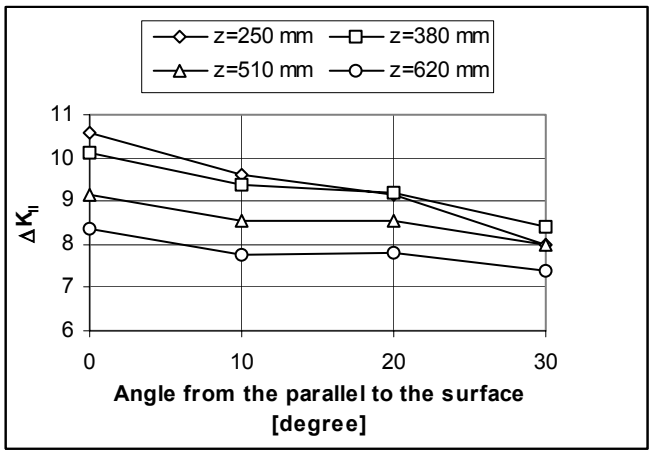

Figure 6: ΔK_{II} versus crack orientation (crack length: 20 μm)

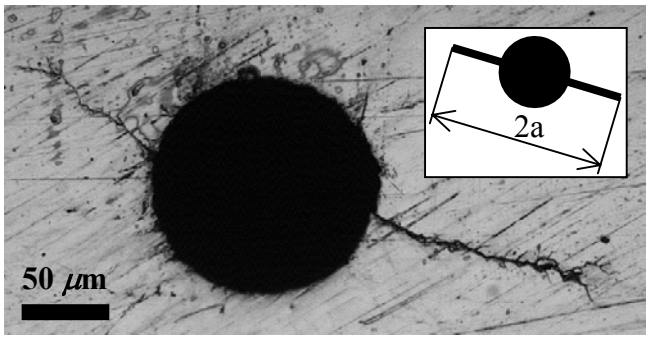

Figure 7: second stage of crack propagation from micro-holes

The cracks propagating from deeper micro-holes (C and D) stopped when they reached a total length 2a (defined as shown in fig.7) of about 250-300 μm, while the cracks propagating from the micro-holes A and B, closer to the surface, continued growing up to $2 \cdot 10^6$ load cycles, after which the test was stopped. In fig.8 the crack length 2a is reported as a function of the cycles number for the four micro-holes. A linear approximation shows that the growth rate is in the range of the threshold.

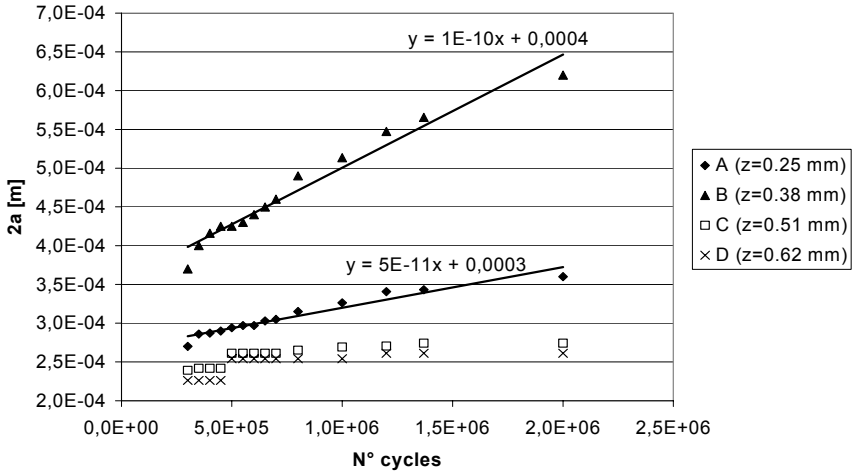

Figure 8: crack growth from micro-holes at different depths

DISCUSSION

In fig.9, the ΔK_{II} for the experimentally propagating and non-propagating cracks, calculated by the fem analyses at the correspondent lengths and orientations, is reported as a function of the total crack length 2a. The first calculations were made for cracks of length 2a=170 μm (i.e. 20 μm from the hole border). In the case of multiple cracks emanating from a hole, those stopped after about 20 μm have been considered as "non-propagating". For the propagating cracks reported in fig.8, further calculations were carried out with increasing length, up to the lenghts observed at the end of the test. For the cracks emanating from holes C and D, the last calculations were made at the length correspondent to their arrest and results were indicated as "non-propagating" in the diagram. In the same figure, for each hole is reported in solid line a curve proposed to describe the mode II threshold [12].

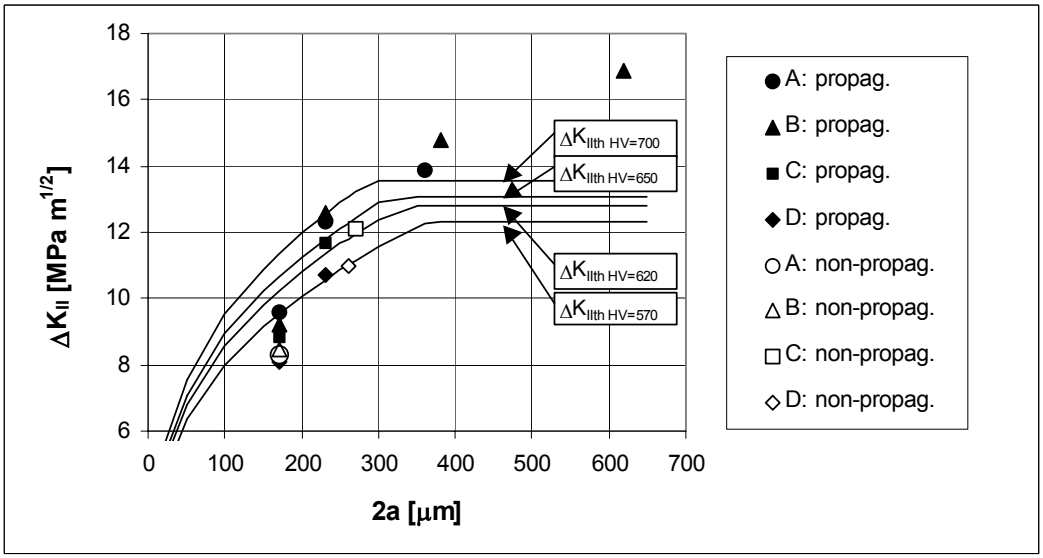

Figure 9: experimental results and proposed threshold curves

Each threshold curve is composed by two parts. The first one, depending on the crack length in the short cracks range:

$$\Delta K_{IIth} = 2.5 \cdot 10^{-3} \cdot (HV + 120) \cdot \left(\sqrt{A}\right)^{1/3} \tag{2}$$

with $\sqrt{A} = 2a$, based on the hypothesis that the influence of hardness and defect dimension on the mode II threshold is the same as the Murakami's mode I relationship (1), where the coefficient 2.5 has been determined on the basis of the study of Beretta et al. [14] on carburised steels. A "closure" effect also in mode II is implicitly hypothesised in this way; it can be mainly attributed to roughness or oxide entrapment between the crack faces. The second one, independent on the crack length in the long cracks range:

$$\Delta K_{IIth} = 6.86 + 9.55 \cdot 10^{-3} \cdot HV \tag{3}$$

based on the study of Kato et al. [15] on carburised steel and the results of Sakae et al. [8], Murakami et al. [10] and Otsuka et al. [6] on hardened steels. It allows to taken in to account the influence of the hardness and also agrees with the results of Hellier et al. [16] and Lunden [17] on carbon steels for rails and railway wheels. The agreement between the present experimental results and the threshold curves proposed above is not so good for smaller cracks: more verifications and refinements, both experimentally (tests with smaller micro-holes) and numerically (3D models) are necessary. From the experimental results, it appears however interesting that smaller cracks seem to present smaller mode II threshold, thus indicating also for this propagation mode a "short cracks" effect. In this sense, the proposed relationships can represent a rough tool to predict the subcase fatigue limit in a rolling contact phenomenon, in terms of the maximum contact pressure which can be applied without determining crack propagation from inherent defects. In particular, for an herztian contact, a propagation index can be defined in the form:

$$I = \frac{\Delta K_{II}(p_0, b, a, z)}{\Delta K_{IIth}(HV(z), a)} \tag{4}$$

where p_o is the nominal contact pressure, b the contact area half-length, 2a the maximum expected defect dimension (which can be evaluated by means of the statistics of extreme values) and HV(z) the hardness profile. A simplified form for ΔK_{II} is [12]:

$$\frac{\Delta K_{II}}{p_0 (\pi a)^{1/2}} = \left(c_0 + c_1 \cdot \frac{z}{b} + c_2 \cdot \left(\frac{z}{b}\right)^2 + c_3 \cdot \left(\frac{z}{b}\right)^3 + c_4 \cdot \left(\frac{z}{b}\right)^4 \right) \tag{5}$$

with $c_0 = 0.21632$; $c_1 = 1.49316$; $c_2 = -2.7232$; $c_3 = 1.97346$; $c_4 = -0.5284$. In fig. 10 is reported an example of the propagation index determination with two different hardness profiles, having equal surface and core levels. Representing I as a function of the depth, it is possible to evaluate the risk of subcase fatigue failure and its location. The strong influence of the hardness profile can be so put in evidence.

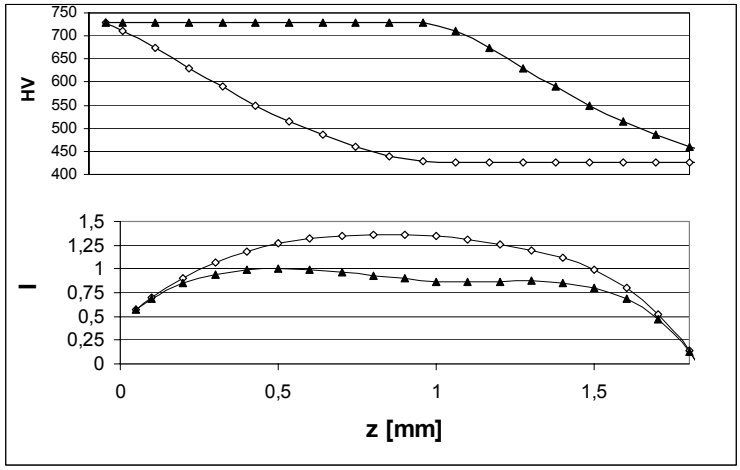

Figure 10: propagation index with different hardness profiles

CONCLUSIONS

- Experimental tests on the carburised disk shown that when the crack extends from the hole border, it passes from a zone dominated by opening stresses (stage I, mode I), to a zone dominated by shear stresses (stage II, mode II). After the first stage, it can therefore continue growing only if $\Delta K_{II} > \Delta K_{IIth}$. This happens preferentially for cracks slightly inclined with respect to the contact surface direction.
- The mode II threshold of the cracks emanating from the micro-holes appears to increase with the crack size, thus indicating a "short cracks" effect also for this propagation mode.
- The proposed "propagation index" allows to take in to account the hardness profile, thus evaluating its effect on the subcase fatigue limit.

References

1. Hyde, R.S. (1996). In: *ASM Handbook*, 19.
2. Voskamp, A.P. (1998). In: *Bearing Steels: Into the 21st Century*, ASTM STP 1327, Hoo & Green (Eds). ASTM.
3. Nelias, D., et al. (1999) *Journal of Tribology* 121, 240
4. Auclair, G., et al. (1997) *5th Int. Symposium on Bearing Steels*, ASTM STP 978. New Orleans.
5. Murakami Y. and Endo, M., (1994) *Fatigue* 16, 163
6. Otsuka, A., Sugawara, H. and Shomura, M. (1996) *Fatigue Fract. Engng. Mater. Struct.* 19, 1265
7. Salehizadeh, H., Saka, N. (1992) *Journal of Tribology* 114, 690
8. Sakae, C., Ohkomori, Y. and Murakami, Y. (1999) Internal report, Kyushu University
9. Melin, S. (1986) *Int. Journal of Fracture* 30, 103
10. Murakami, Y., Sakae C., Hamada S. (1999). In *Mechanism of Rolling Contact Fatigue and Measurement of ΔK_{IIth} for Steels, Engineering Against Fatigue* Beynon et al. (Eds). A.A. Balkema. Rotterdam & Brookfield.
11. Pook, L.P. (1989) In: *Biaxial and Multiaxial Fatigue*, EGF 3, Brown & Miller (Eds), Mechanical Engineering Publications.
12. Donzella G., Mazzù A., Pola A., Solazzi L. (2000) *Atti XXIX Conv. Nazionale AIAS*, Lucca, pp.407-416.
13. Melander, A. (1997) *Int. Journal of Fatigue* 19, 13
14. Beretta, S., Clerici, P. and Guagliano, M. (1998) *XXVII Convegno Nazionale AIAS,* Perugia, pp.249-258
15. Kato, M., Deng, G., Inoue, K. and Takatsu, N. (1993) *JSME Int. Journal* 36, 233
16. Hellier, A.K., McGirr, M.B. and Corderoy, D.J.H. (1991) *Wear* 144, 289
17. Lunden, R. (1992) *Int. Wheelset Congress*, Sydney, pp.163-167